

Supporting Information

for

Chiral hybrid inorganic-organic materials: synthesis, characterization and application in stereoselective organocatalytic cycloadditions*

Alessandra Puglisi,* Maurizio Benaglia, Rita Annunziata, Valerio Chiroli, Riccardo Porta and Antonella Gervasini

Dipartimento di Chimica, Università' degli Studi di Milano – via Golgi 19, I-20133 Milano, Italy

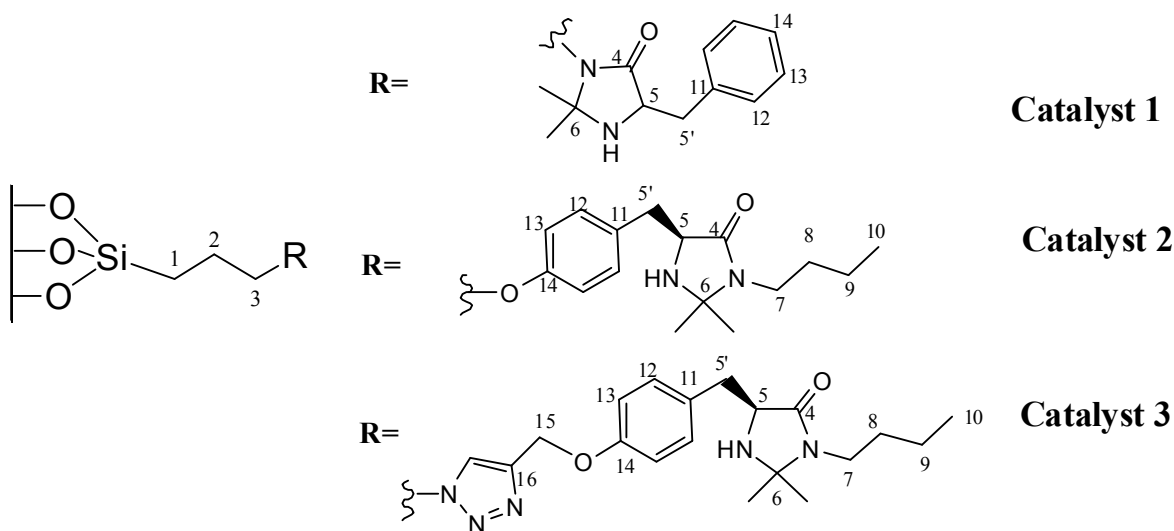
E-mail: alessandra.puglisi@unimi.it

Table of Contents:

¹³ C CPMAS NMR of catalysts 1-4	page 2
²⁹ Si MAS NMR of catalysts 1-4	page 3
BET isotherms and BJH distribution of compounds 3 and 13	page 7
¹ H-NMR spectrum of compound 15	page 9
¹ H-NMR spectrum of reduced compound 15	page 10
¹ H-NMR spectrum of entry 1 Table 2	page 11
¹ H-NMR spectrum of entry 4 Table 2	page 12
¹ H-NMR spectrum of reduced entry 4 Table 2	page 13
HPLC spectrum of reduced compound 15	page 14
HPLC spectrum of reduced entry 2 Table 2	page 15
HPLC spectrum of reduced entry 4 Table 2	page 16
HPLC spectrum of reduced entry 3 Table 2	page 17
GC spectrum of reduced entry 1 Table 2	page 18
SEM of bare silica and catalyst 2	page 19

¹³C CPMAS NMR of catalysts 1-4.

The ¹³C spectra of catalysts **1-4** demonstrated that the mesopores were indeed functionalized as expected and the organic residues were stably bounded to the inorganic material (see the chemical shifts of C-1 and C-3 carbons). The ¹³C resonances in Table 1 are assigned based on the chemical shifts found in the solution spectra of organic precursor.



	1	2	3	5	11	12	13	14	14	15	16
1	9.2	20.0	49.4	58.5	136.2	128.0	128.0	128.0	128.0		
2	7.7	22.4	70.0	60.0	129.9	129.6	114.4	158.1	158.1		
3	9.0	23.0	51.8	58.0	129.0	129.0	114.0	157.4	157.4	62.0	143.3

The resonances of following carbons are the same for all compounds: C-4 174.0, C-6 76.0, C-5' 40.0, C-7 50.0, C-8 28.0, C-9 19.7, C-10 13.0 ppm

Table 1. Selected ¹³C NMR resonances shown in the solid state spectra of catalysts **1-3**

It should be noted that the ¹³C spectrum of catalyst **3**, synthesized by cycloaddition of imidazolidinone **14** with the supported azide **13**, revealed 25% of unreacted azide starting material; indeed the recovered mesoporous silica catalyst **3** is a bi-functionalized material. It was possible to

calculate the ratio of two organic moieties from the integration of C-1 (9.0 ppm) and C-10 (13.0 ppm) signals; moreover the high intensity of signal at 50.0 ppm confirmed the presence of the carbon corresponding to $\underline{\text{C}}\text{H}_2\text{N}_3$ group.

As a consequence, the ^{13}C spectrum of TMS-capped catalyst **4**, synthesized from **3**, revealed the presence of three substituents: the azide and imidazolidinone chains, already present in the starting material **3**, and the new introduced SiMe_3 group, with a roughly ratio of 37.5: 12.5: 50.0, respectively.

²⁹Si DP and CPMAS NMR.

The ²⁹Si solid state spectra of catalysts **1-3** (Figure 1) are dominated by resonance lines at -113, -103 and -96 ppm representing silicon sites Q₄, Q₃ and Q₂, respectively. Moreover, the spectra clearly showed very different patterns for the functionalized T_n species, where the silicon atoms are directly bound to at least one organic moiety. The figure displays the characteristic resonance frequencies at -68 ppm for the T₃ species [(SiO)₂ SiR'(OX) with X =H or Et] and upfield resonance at -60 ppm related to T₂ forms [(SiO)SiR(OX)₂], traces of T₁ at -54 ppm were detected only for catalyst **1**; the ¹³C spectrum confirmed the presence of T₁ form showing a large resonance at 50.0 ppm. The ²⁹Si solid state spectra of catalyst **4** was similar to that of catalyst **3** and, in addition, it showed the peculiar resonance peak of the SiMe₃ group at 10.6 ppm.

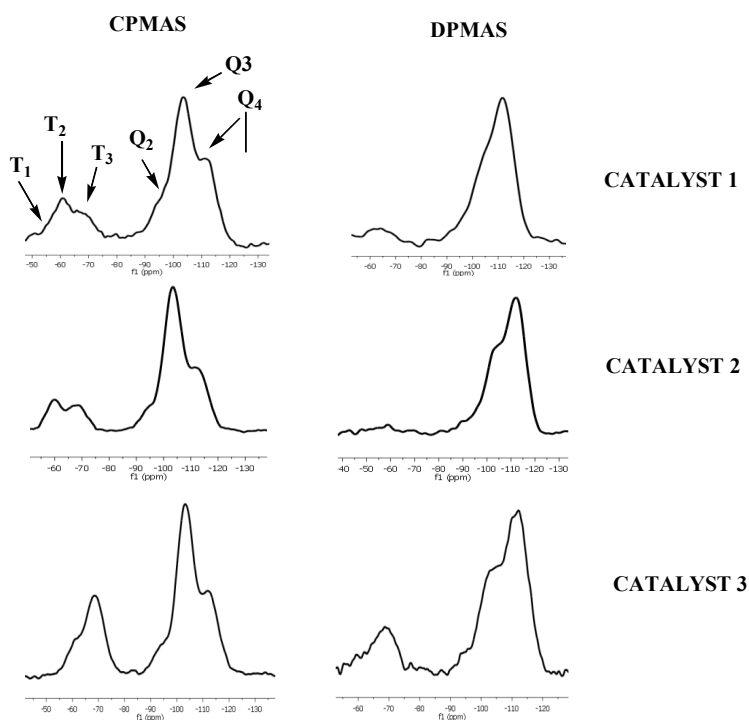


Figure 1. ²⁹Si CPMAS (left column) and DPMAS (right column) NMR spectra obtained for mesoporous catalysts **1-3**.

The presence of peaks assigned to T_3 , T_2 and T_1 showed that the organic groups are indeed covalently bound to the surface. In spite of the better sensitivity of ^{29}Si spectra recorded by cross-polarization (CP) technique, quantitative measurements of T_n and Q_n silicon groups could be properly achieved by ^{29}Si DP/MAS experiments, except for compound **4** because of the very low sensitivity of its ^{29}Si DP spectrum. Accordingly, deconvolution analysis of ^{29}Si DP spectra of catalysts **1-3** were performed to recognize T_n and Q_n relative concentrations, surface coverage and molar concentrations of organic moieties; the data are reported in Table 2.

TABLE 2. ^{29}Si DP/MAS NMR Chemical Shifts, relative concentrations of T_n and Q_n silicon groups (in %), surface coverage (SC, in %, see text for explanation) and molar concentrations of organic moieties (MC) of catalysts **1-3**

CATALYST	T_1 % -54 ppm	T_2 % -60 ppm	T_3 % -68 ppm	Q_2 % -96 ppm	Q_3 % -103 ppm	Q_4 % -113 ppm	SC (%)	MC (mmol/g)
1	1.8	4.9	2.1	8.3	23.9	59.0	21.4	1.02
2	-	3.9	1.1	9.1	29.1	56.8	11.6	0.62
3	-	4.1	13.0	4.4	30.5	48.0	33.0	1.43 ^b
4^a	-	2.2	8.5	4	21.1	52.7	29.9(46.9 ^c)	

^a) Calculated from ^{29}Si CP/MAS spectra; ^b) overall (catalyst + azide); ^c) this SC value includes the SiMe_3 substituent

Based on the deconvolution analysis of the ^{29}Si DP/MAS spectra (Table 2), we estimated that an amount from 5.0 to $17.1 \pm 2\%$ of silicon atoms in these samples are bound to carbon, but this percentage remarkably increases (from 15.9 to $19.8 \pm 2\%$) when we performed the deconvolution employing the ^{29}Si CPMAS spectra; as expected, in this case the $^1\text{H} \rightarrow ^{29}\text{Si}$ cross-polarization increases the resonance intensities of the silicon atoms that are in proximity of protons, thus enhancing the percentage of the substituted T_n forms with respect to the unsubstituted Q_n .

It is immediately apparent that introducing imidazolidinone derivative **14** on the supported azide **13** to give catalyst **3** is a good strategy, compared to the grafting method used for the synthesis of catalyst **1** and **2**, to produce a wider distribution of T_n species. Assuming that all Q_2 and Q_3 sites are

located on the interior walls of mesoporous silica, the surface coverage (SC) of mesopores with organic moieties could be estimated as $(T_1 + T_2 + T_3) / (Q_2 + Q_3 + T_1 + T_2 + T_3)$. The SC values are 21.4 and 11.6%, for catalysts **1** and **2**, respectively, and SC raises to 33.0 % for catalyst **3**. The SC decrease found passing from **1** to **2** can be ascribed to a major steric requirement of **2** which inhibits the condensation reaction.

At the lowest siloxane coverage (catalyst **2**, SC = 11.6%) the T_2 components are prevalent; by increasing the siloxane content, the T_2 decreases and a significant percentage of T_3 structure arises in catalyst **3**: silicon atoms are progressively involved in one, two, and three bonds increasing the siloxane coverage.

Morphological properties of compounds **3** and **13**

The textural properties in terms of surface areas, pore volumes, and pore size distributions of the azide **13** and catalyst **3** have been determined by N₂ adsorption-desorption isotherms. The two surfaces have characteristic type IV BET isotherms consistent with the presence of cylindrical meso-scale pores (Fig. 2). The BET surface areas of **13** and **3** are of 1109 and 486.5 m²·g⁻¹, respectively. The loss of surface area observed for catalyst **3** could be due to the higher density of the organic functionalities loaded on the azide sample which completely cover the silica surface. Concerning porosity, for both samples, the hysteresis region between the adsorption and desorption isotherms closes at low relative pressure (P/P₀=0.90), indicating the presence of small sized pores (Table 3). A clear step can be noted in the adsorption isotherms, in particular for azide sample **13**, in the relative pressure range 0.25–0.35, corresponding to capillary condensation in the mesopores.

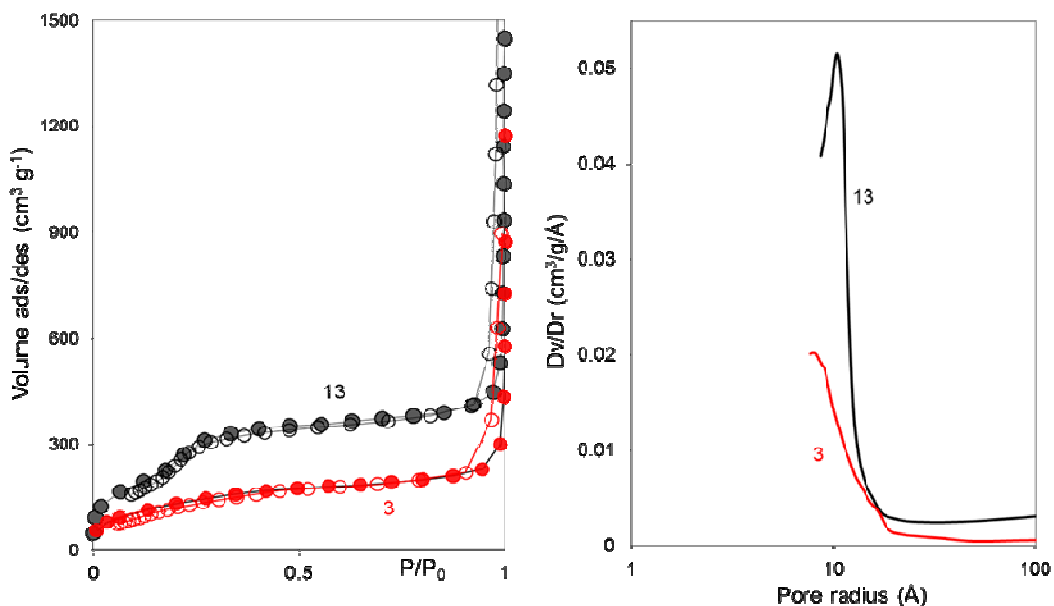


Figure 2. N₂-adsorption (full marks) and desorption (open marks) isotherms collected at -196°C (left) and calculated pore size BJH distribution curves (right) of **13** and **3** samples.

The pore size distribution calculated by the BJH approach, showed a defined pore population around 20 Å and 16 Å of size for **13** and **3**, respectively. It is interesting to observe that the total pore volume halves passing from **13** to **3** (Table 3). Azide **13** has little more than twice the surface than catalyst **3** and more than three times the pore volume. This means that catalyst **3** has smaller

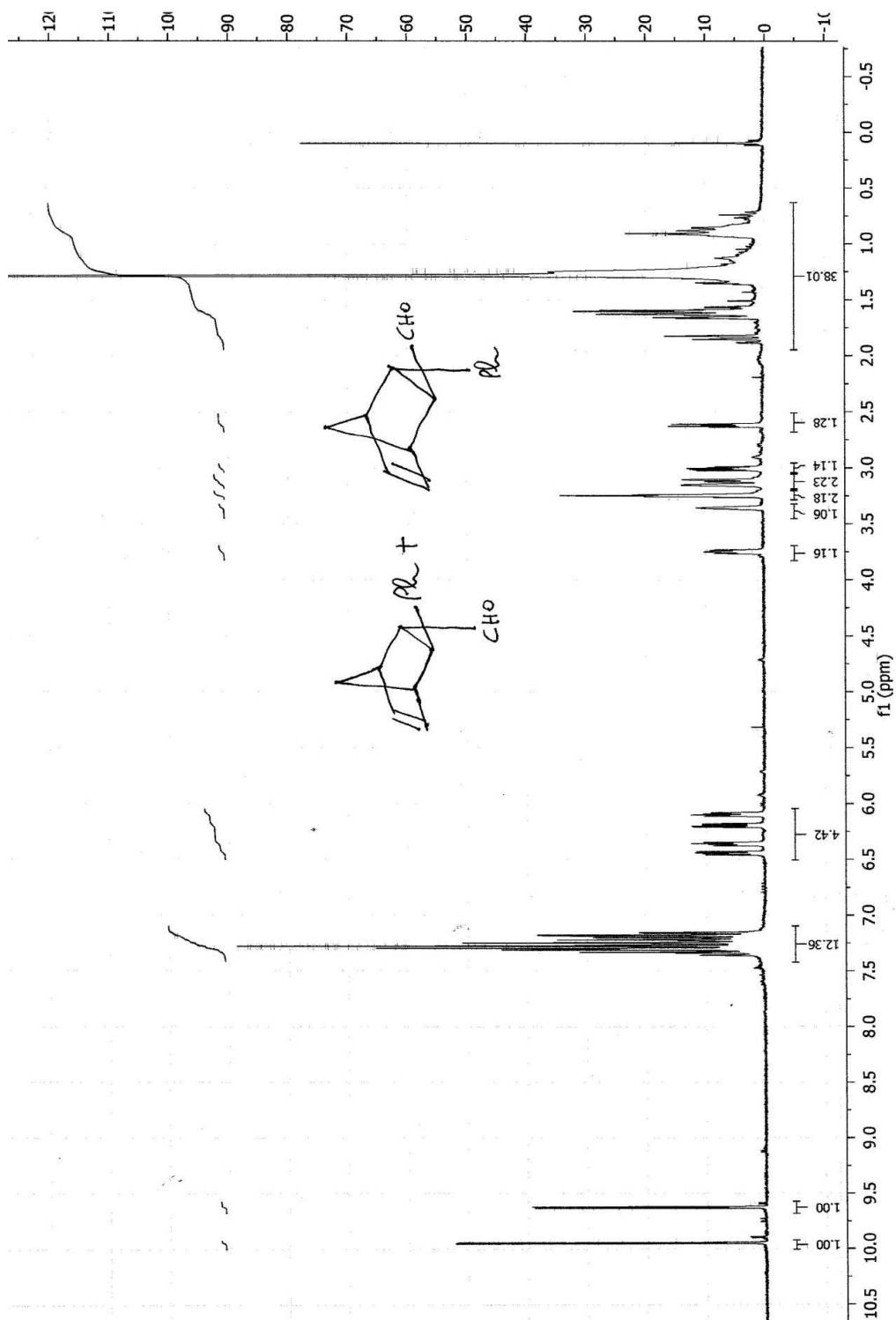
pores of azide **13** (as confirmed by the BJH pore size distribution). The strong decrease of both surface area and pore volume observed for catalyst **3** is likely due to the high loading of the organic functionalities which can be housed in the pores of silica, too. Some morphologic differences emerged between the previous studied hybrid materials and the new samples (azide **13** and catalyst **3**). Both **3** and **13** have much higher porosity (pore volume) than the already studied silica particles carrying tertiary amine and thiourea residues¹⁶ and they have unique pore population. The observed differences between the two sample series could be ascribed to the different nature and structure of the organic functionality loaded on silica which has been accommodated at the open surface rather than into the silica pores in azide **13** and catalyst **3** samples.

Table 3 Main morphological properties of the synthesized hybrid materials.

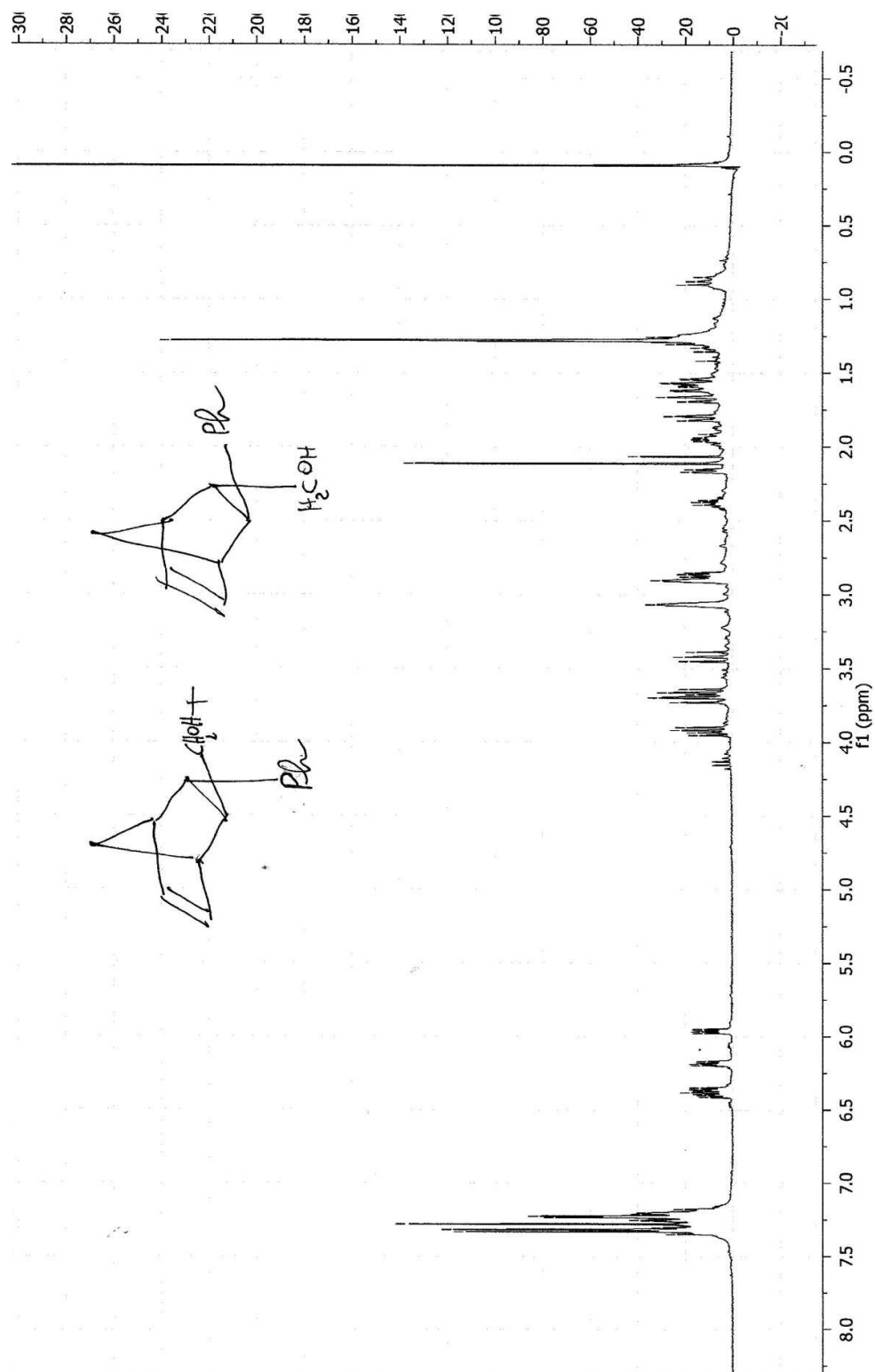
Sample	N ₂ uptake [cm ³ (STP)·g ⁻¹]	Surface Area [m ² /g]	Total Pore Volume [cm ³ /g]	Average Pore Size [Å]
Azide 13	254.7	1109	1.28	20
Catalyst 3	111.8	486.5	0.461	16

NMR spectra:

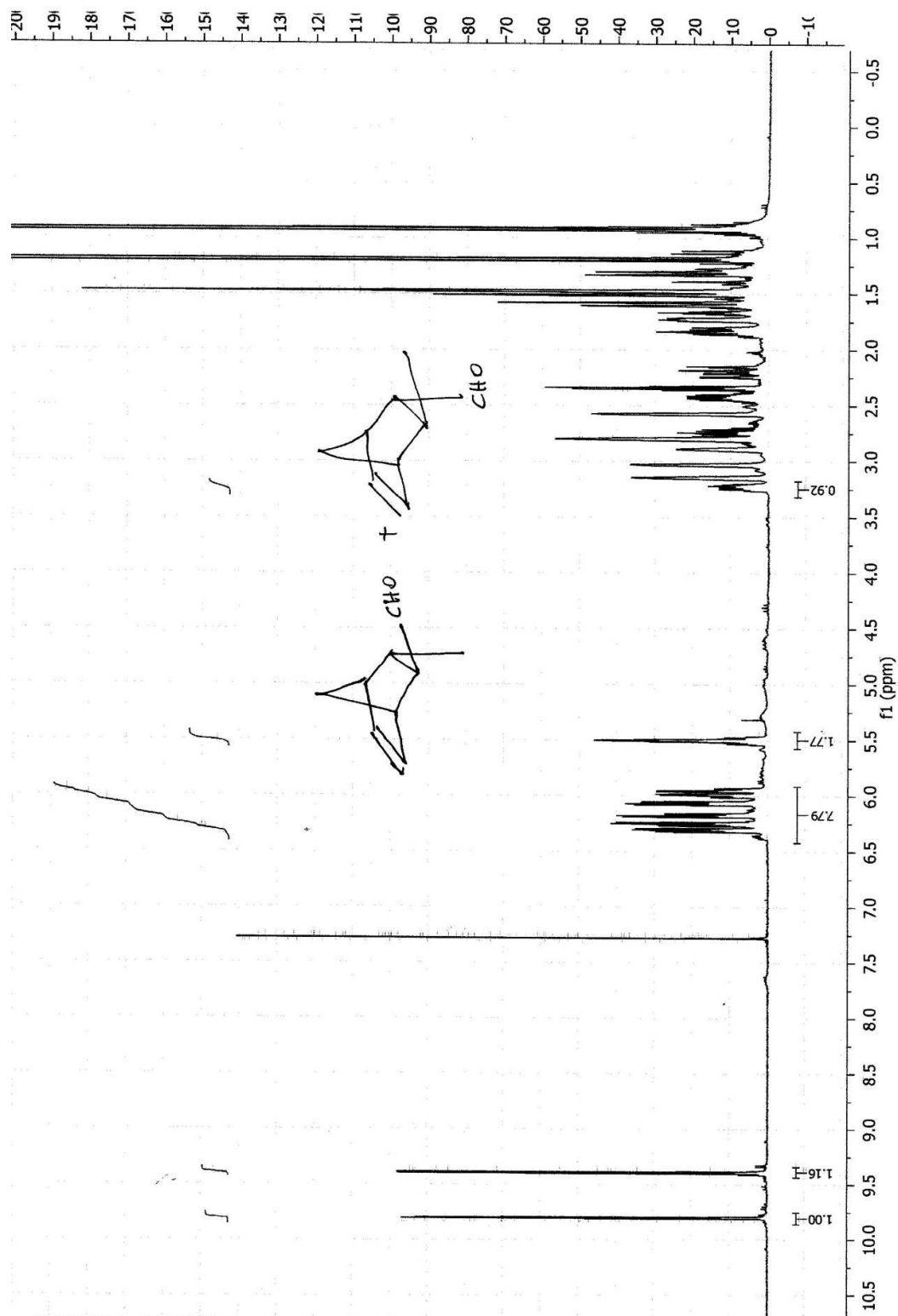
1) ^1H NMR of *endo*-15 + *exo*-15



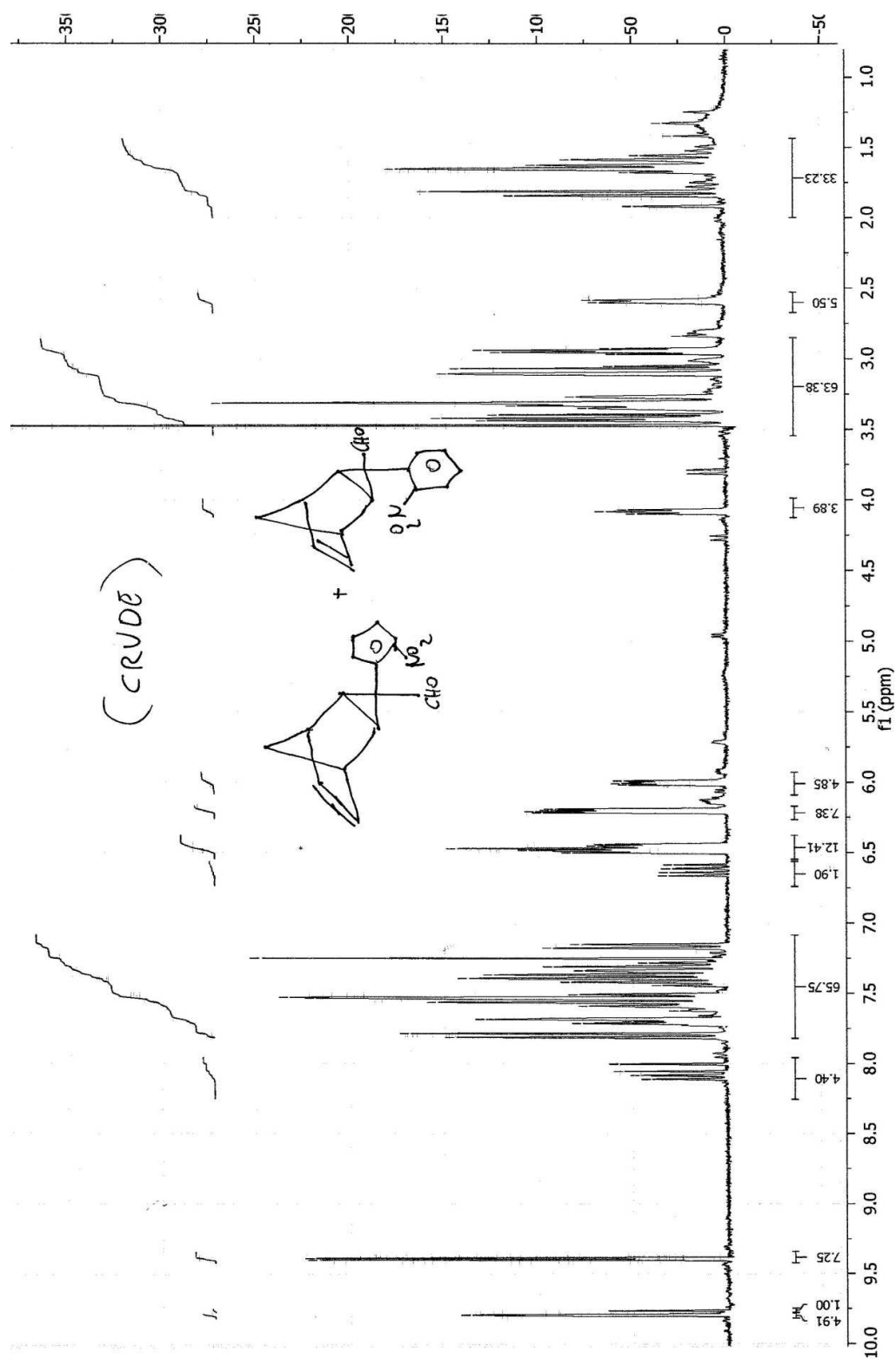
2) ^1H NMR of REDUCED *endo*-15 + *exo*-15



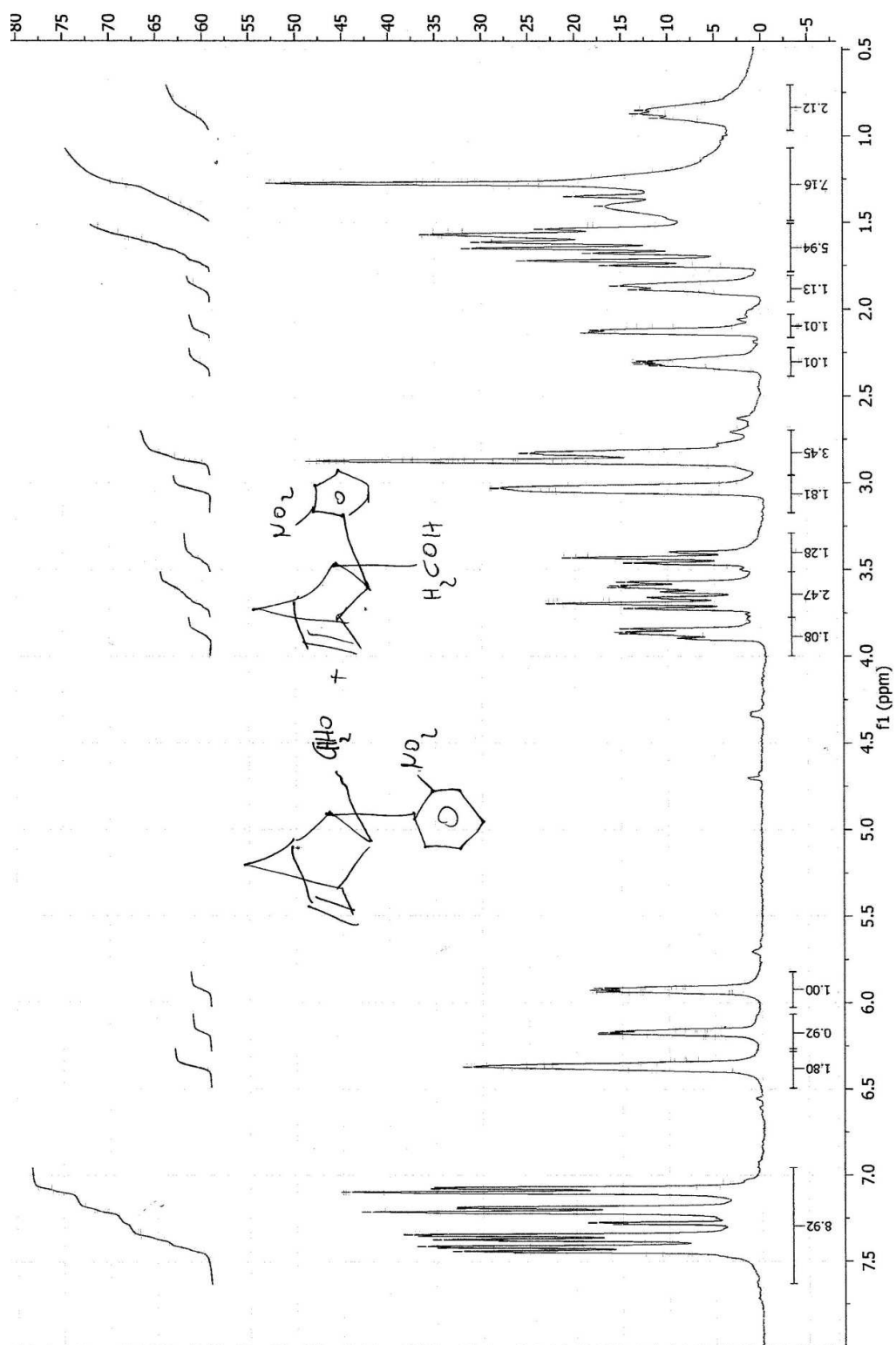
3) ^1H NMR of entry 1 Table 2 (mixture of diastereoisomers)



4) ^1H NMR of entry 4 Table 2 (mixture of diastereoisomers)

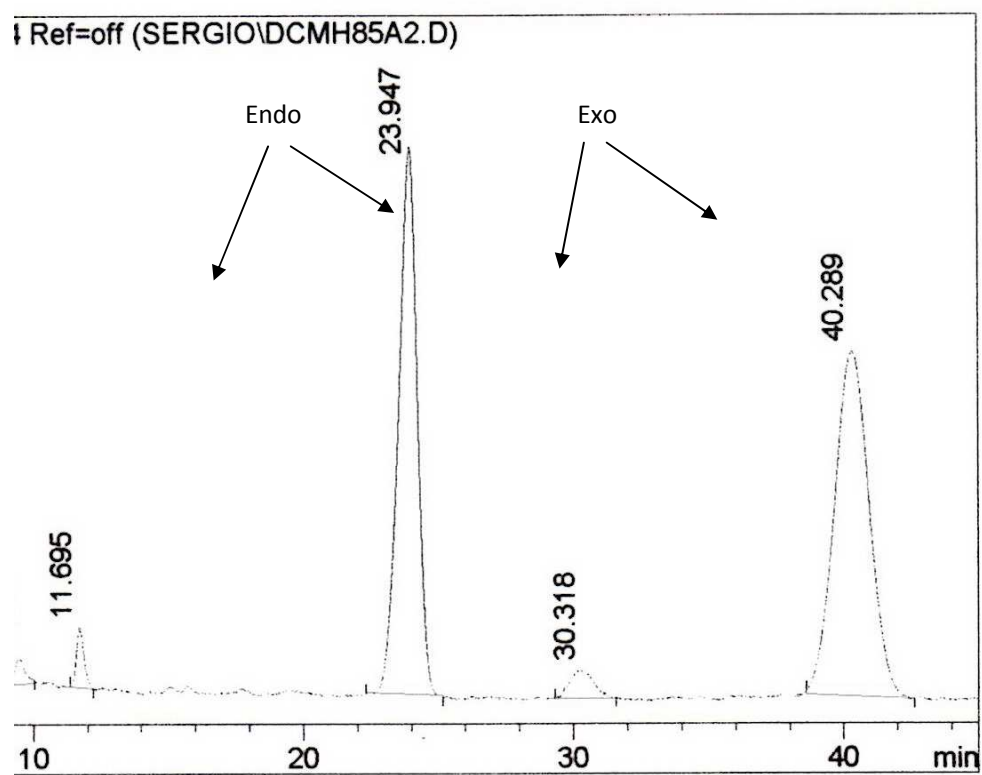


5) ^1H NMR of reduced entry 4 Table 2 (mixture of diastereoisomers)



HPLC spectra:

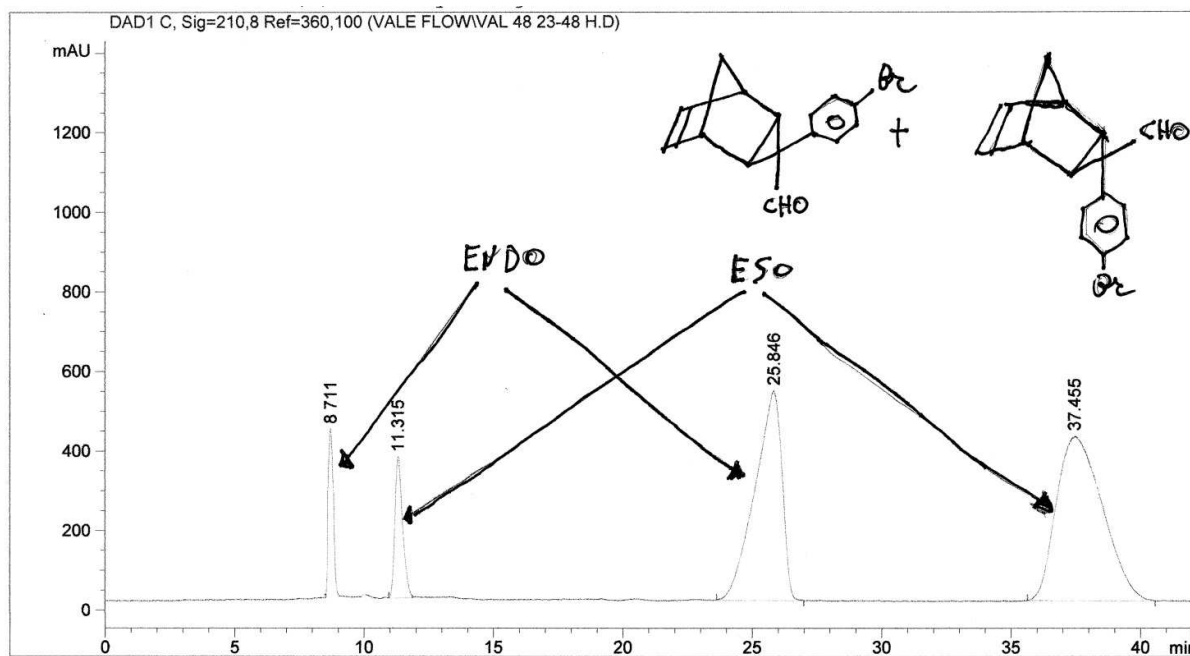
1) Reduced compound 15



2) Reduced entry 2 Table 2

The enantiomeric excess was determined on the alcohol by HPLC on chiral stationary phase (Chiralcel OJ-H, flow 0.8 mL/min, pressure 43 bar, Hexane/2-Propanol = 90/10).

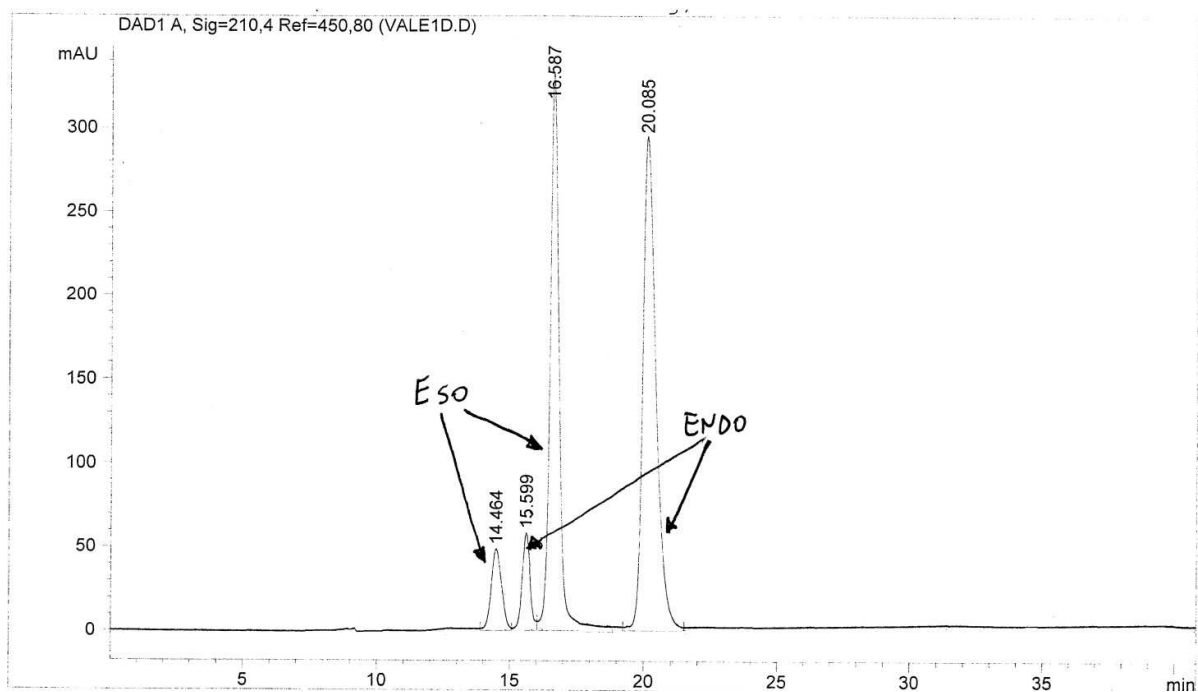
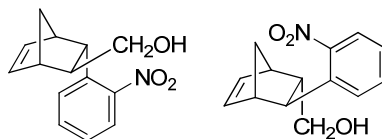
Endo isomer $t_R = 8.7$ min; $t_R = 11.3$ min; *Exo* isomer $t_R = 25.8$ min; $t_R = 37.4$ min.



3) Reduced entry 4 Table 2

The enantiomeric excess was determined on the alcohol by HPLC on chiral stationary phase (Chiralpack AD, flow 0.8 mL/min, pressure 17 bar Hexane/2-Propanol = 95/5).

Exo isomer $t_R = 14.5$ min; $t_R = 16.6$ min; *Endo* isomer $t_R = 15.6$ min; $t_R = 20.1$ min.



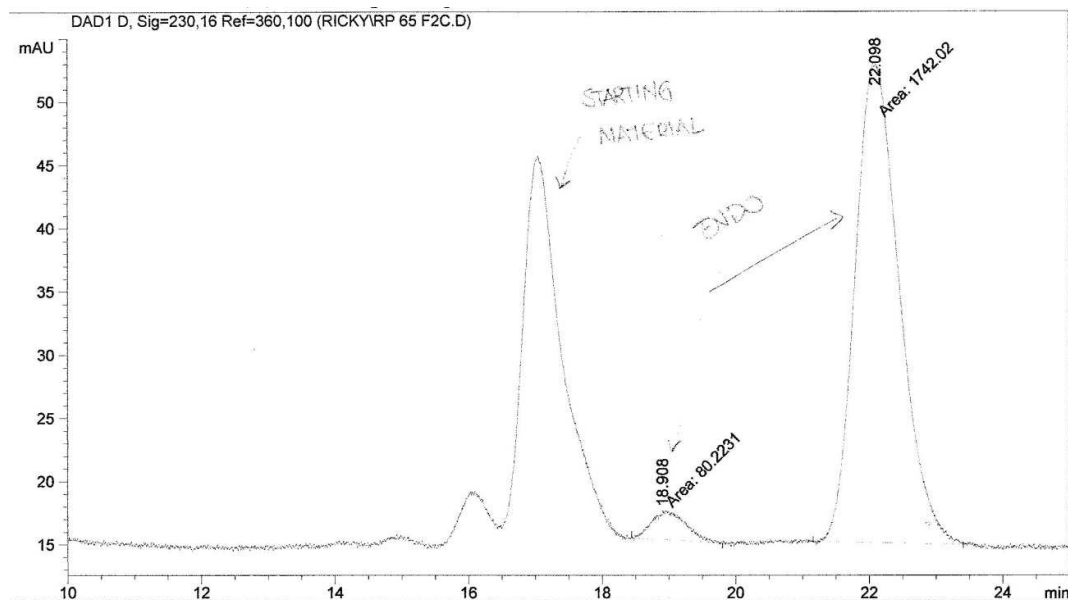
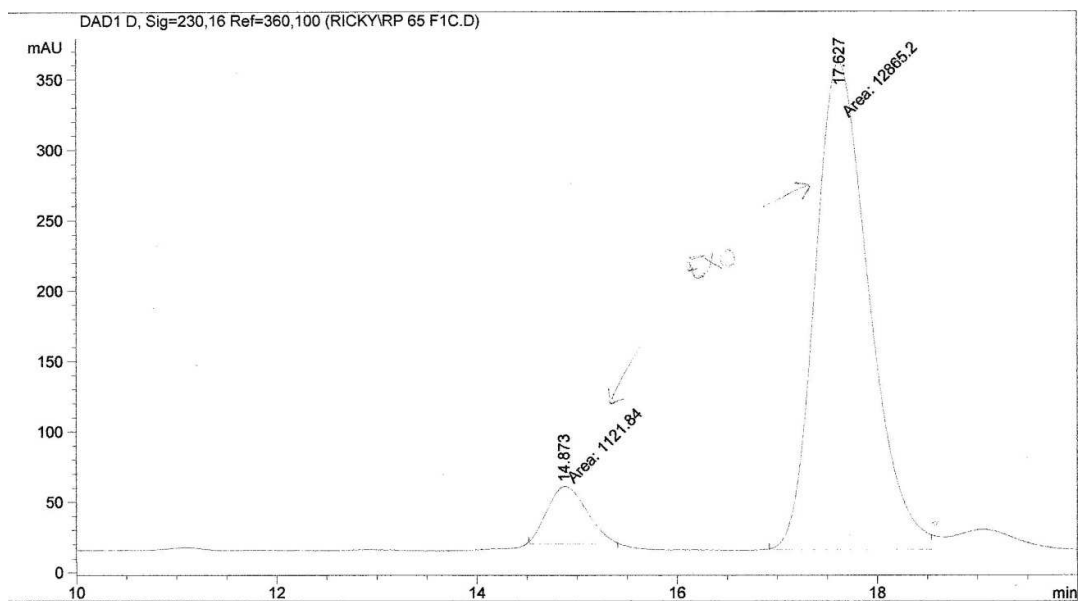
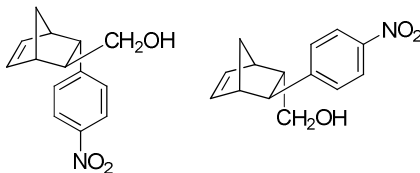
4) Reduced entry 3 Table 2

The enantiomeric excess was determined on the alcohol by HPLC on chiral stationary phase (Chiralpack AD, flow 0.8 mL/min, pressure 17 bar Hexane/2-Propanol = 95/5).

The two enantiomers were separated by column chromatography and injected separately.

Exo isomer (fraction 1) $t_R = 14.9$ min; $t_R = 17.6$ min;

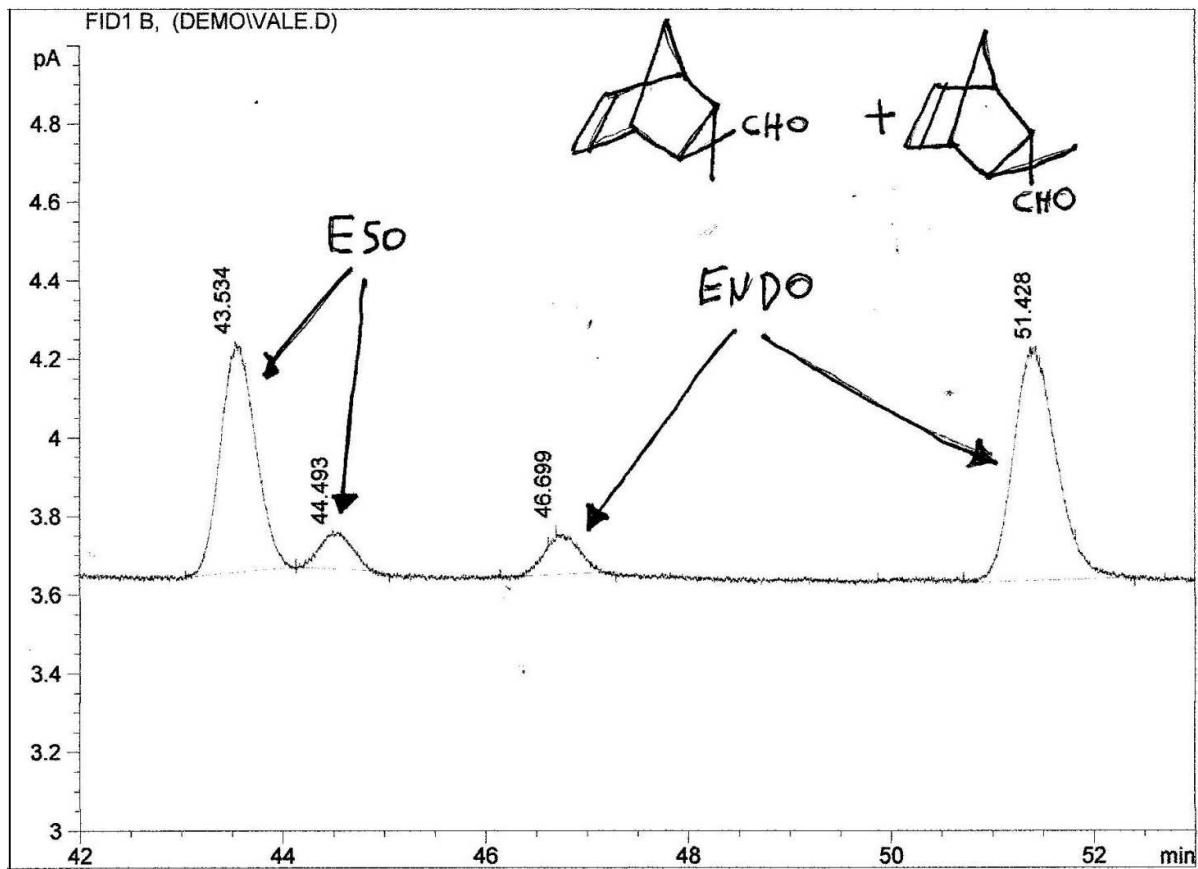
Endo isomer (fraction 2) $t_R = 18.9$ min; $t_R = 22.0$ min.



GC spectrum of reduced entry 1 Table 2

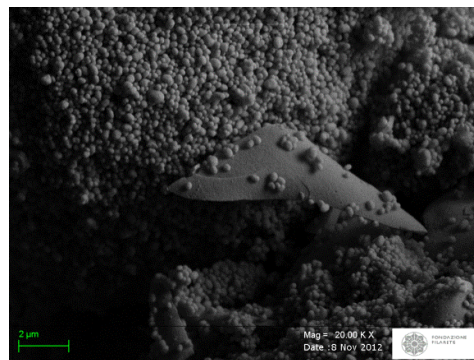
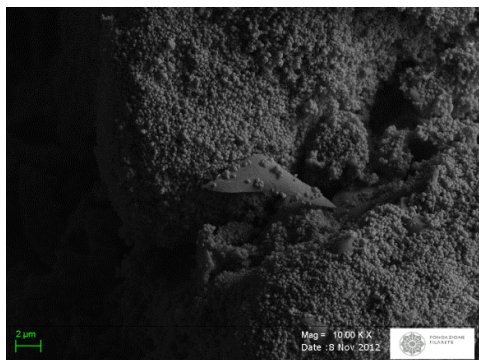
The enantiomeric excess was determined on the aldehyde by gas chromatography on chiral stationary phase (20% permethylated β -cyclodextrine, oven temperature = 75°C, He flow = 2 mL/min, pressure = 2 bar).

Exo isomer t_R = 43.5 min; t_R = 44.5 min; *Endo* isomer t_R = 46.7 min; t_R = 51. min.



SEM images

Scanning Electron micrographs of bare silica prepared from TEOS in the presence of CTAB in NaOH solution: the MSNs show a spherical morphology



Scanning Electron micrographs of catalyst **2** prepared from bare silica: the MSNs maintain the spherical morphology of the precursor silica.

